Progress In Electromagnetics Research C, Vol. 29, 249–260, 2012

NOVEL CLASS OF MICROSTRIP BANDPASS FILTERS WITH IMPROVED UPPER REJECTION BAND

Y.-L. Lu and G.-L. Dai*

Department of Information Science and Electronic Engineering, Zhejiang University, Hangzhou 310027, China

Abstract—In this paper, we present a novel class of microstrip bandpass filters with improved upper rejection band. The proposed filters are composed of two half-wavelength resonators and two short-ended microstrip feed lines for input and output. Using voltage-wave analysis, we examine the resonance and coupling properties at harmonic frequencies. It is found that different combinations of the feed line and the resonator with proper selection of the coupling regions can suppress spurious responses. Benefiting from this approach, two single-band and one dual-band bandpass filters are designed, fabricated and measured. Simulated and measured results indicate that the upper rejection bands of the proposed filters are increased up to near third- and fifth-order harmonics, respectively. And the rejection level during the stop-bands is more than 20 dB.

1. INTRODUCTION

Microstrip bandpass filter is one of the most important components in wireless communication systems [1–3]. Unfortunately, without special measures, most of the microstrip BPFs exhibit harmonic responses degrading the system performance. To overcome this problem, various methods have been presented in the past [4–20]. Among them, modification and perturbation to the width of the coupled-line resonators are the most widely used approach to suppress the spurious response [4–7]. However, these filter designs only focus on the second harmonic suppression. To obtain wide-stopband, stepped-impedance resonators (SIRs) are proposed [11–16]. In [11–15], SIRs with high frequency ratios and proper tapping locations are utilized to obtain

Received 14 March 2012, Accepted 26 April 2012, Scheduled 29 May 2012

* Corresponding author: Gao-Le Dai (daigl@zju.edu.cn).

wide-stopband. In [16], a combination of different SIR structures with the same fundamental resonance frequency but diverse spurious resonances is adopted for spurious-suppressed BPFs.

Recently, the authors have presented a new method to design harmonic-suppressed bandpass filters [17]. We combined open- and short-ended resonators together and chose the proper coupling region between them for spurious suppression. In [18, 19], an extended research of the proposed special coupling region is analyzed. The combination of open-ended resonators is employed to suppress the second harmonic. Based on our further investigation, coupling characteristics between the short-ended feed line and the resonator are studied. It is found that special coupling region not only between resonators, but also between feed line and resonator can be used to suppress the harmonic. This property provides more convenience to employ different resonators for harmonic-suppressed filter designs.

In this paper, we present a novel class of microstrip bandpass filters with improved upper rejection level. The proposed filters are both composed of two half-wavelength resonators and two-shorted feed lines for I/O ports. Using voltage-wave analysis, the coupling properties between the resonator and the feed line are examined. It is found that different combinations of the feed line and the resonator with proper selection of the coupling regions can suppress spurious responses. Loading resistor or capacitor at the center of the half-wavelength resonator, both single- and dual-band responses with harmonic suppression can be obtained. Three demonstration filters are implemented to validate the proposed idea. Simulated and measured results indicate that the upper rejection bands of the proposed filters are increased up to near third- and fifth-order harmonics, respectively. And the rejection level during the stop-bands is more than 20 dB.

2. COUPLING PROPERTIES BETWEEN THE HALF-WAVELENGTH RESONATOR AND THE FEED LINE

As discussed in [20], the coupling coefficient between coupled structures can be defined on the basis of the ratio of coupled energy to stored energy, i.e., for equations,

$$k = k_e + k_m \tag{1a}$$

where,

$$k_e = \frac{\int\int\int \epsilon \vec{E}_1 \vec{E}_2 dv}{\sqrt{\int\int\int \epsilon |\vec{E}_1|^2 dv \times \int\int\int \epsilon |\vec{E}_2|^2 dv}} \tag{1b}$$

$$k_m = \frac{\int\int\int \mu \vec{H}_1 \vec{H}_2 dv}{\sqrt{\int\int\int \mu |\vec{H}_1|^2 dv \times \int\int\int \mu |\vec{H}_2|^2 dv}} \tag{1c}$$

Here k_e and k_m represent the electric and magnetic coupling coefficients, respectively. And $\vec{E}_1$, $\vec{E}_2$, $\vec{H}_1$ and $\vec{H}_2$ are the electric and magnetic field vectors of two coupling elements. The volume integrals are over all effected regions with permittivity of ϵ and permeability of μ.

Based on the transmission line theory, the dominant mode can be regarded as quasi-TEM. Then, electromagnetic field associated with the transmission line can be simplified to voltage- and current-wave functions. For parallel coupled microstrip lines, Equations (1b) and (1c) are changed to

$$k_e = P_e \times \frac{\int V_1(l) V_2(l) dl}{\sqrt{\int |V_1(l)|^2 dl \times \int |V_2(l)|^2 dl}} \tag{2a}$$

$$k_m = P_m \times \frac{\int I_1(l) I_2(l) dl}{\sqrt{\int |I_1(l)|^2 dl \times \int |I_2(l)|^2 dl}} \tag{2b}$$

where P_e and P_m are constants and V_1, V_2, I_1 and I_2 are the voltage- and current-wave functions along the coupled lines. And the limit of the line integrals is just the coupling region between two coupled lines.

In [17], the authors have discussed that trigonometric functions can be used to express the voltage-wave function along the open- and short-ended microstrip line resonators. Then, the normalized voltage at the second harmonic of the proposed resonator, shown in Fig. 1(a), can be expressed as

$$V_1 = \cos 2\beta_0 l \quad l \in [0, L] \tag{3}$$

β_0 is the propagation constant at the fundamental resonant frequency.

As presented in [21], the voltage- and current-wave functions along the open-ended feed line can also expressed by trigonometric functions. Therefore, with different terminal condition, voltage-wave function along the short-ended feed line at the second harmonic is given by

$$V_2 = \sin\left[-2\beta_0\left(l - \frac{1}{2}L\right)\right] \quad l \in \left[\frac{1}{2}L, L\right] \tag{4}$$

In the same manner, the normalized voltage at the third harmonic of the proposed resonator is

$$V_3 = \cos 3\beta_0 l \quad l \in [0, L] \tag{5}$$

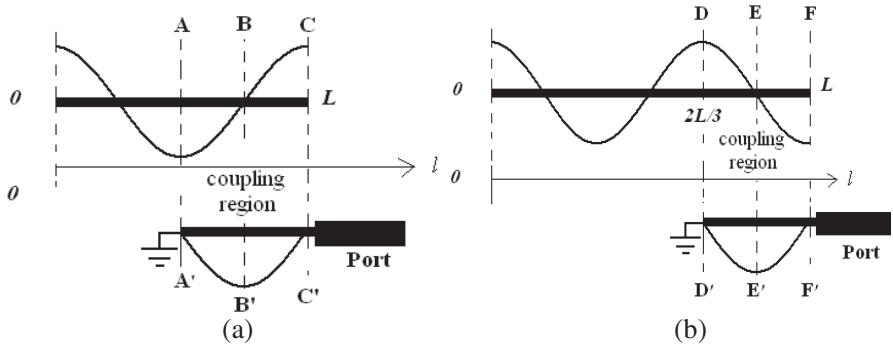

Figure 1. Normalized voltage wave along the proposed resonator and the short-ended feed line. (a) The second harmonic. (b) The third harmonic.

And the voltage-wave function along the short-ended feed line at the third harmonic is given by

$$V_3 = \sin\left[-3\beta_0\left(l - \frac{2}{3}L\right)\right] \quad l \in \left[\frac{2}{3}L, L\right] \tag{6}$$

The curves of the Equations (5) and (6) are shown in Fig. 1(b).

Based on the analysis above, a special coupling region can be employed to suppress the second harmonic as shown in Fig. 1(a). It is from AA' to CC', with respect to the symmetry line BB'. It is easily observed that $V_1(l)$ is an odd function and $V_2(l)$ is an even function with respect to the symmetry line BB'. Thus, the electrical coupling coefficient is

$$k_e = P_e \times \frac{\int_{\frac{L}{2}}^{L} V_1(l)V_2(l)dl}{\sqrt{\int_{\frac{L}{2}}^{L} |V_1(l)|^2 dl \times \int_{\frac{L}{2}}^{L} |V_2(l)|^2 dl}} = 0 \tag{7}$$

As the integrand is an odd function, it yields a zero value upon integration. Similarly, the magnetic coupling coefficient is

$$k_m = 0 \tag{8}$$

Thus, the total coupling coefficient is

$$k = k_e + k_m = 0 \tag{9}$$

The coupling coefficient k of the second harmonic is zero, which also means that the RF signal at the second harmonic cannot be transmitted through the special coupled lines. Similarly, another special region can be adopted to suppress the third harmonic. As

shown in Fig. 1(b), the selected coupling region is from DD' to FF' with respect to the symmetry line BB'. This indicates that the RF signal at the third harmonic can not be transmitted through the special coupling region.

3. FILTER DESIGN

3.1. Bandpass Filter with Second Harmonic Suppression

Based on the analysis above, a bandpass filter with second harmonic suppression is designed in this section. The configuration of the proposed filter is illustrated in Fig. 2. It consists of two folded microstrip half-wavelength resonators and two short-ended feed lines. Two shorting vias are located at the terminals of the microstrip feed lines. The first special coupling region shown in Fig. 1(a) is employed in this structure to suppress the second harmonics.

The experimental filter is fabricated on the substrate with a relative dielectric constant $\epsilon_r = 2.33$ and total thickness of 0.787 mm. The dimensions are shown as follows: $L_1 = 12\,\text{mm}$, $L_2 = 10\,\text{mm}$, $L_3 = 9\,\text{mm}$, $W_1 = 0.5\,\text{mm}$, $W_2 = 2.3\,\text{mm}$, $g_1 = 0.2\,\text{mm}$. The photograph of the proposed filter is shown in Fig. 3. The simulation of this design was accomplished by using Ansoft HFSS. The fabricated prototype was measured by a ROHDE & SCHWARZ ZVA 50 network analyzer. The simulated and measured results are compared in Fig. 4, which shows a good agreement. The center frequency of the passband is measured at

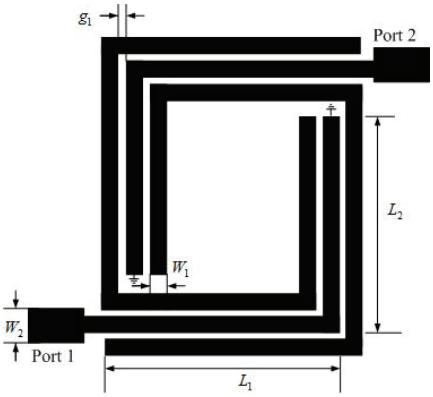

Figure 2. Configuration of the proposed filter with second harmonic suppression.

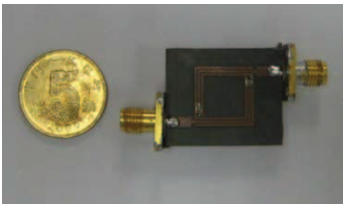

Figure 3. The photograph of the proposed filter with second harmonic suppression.

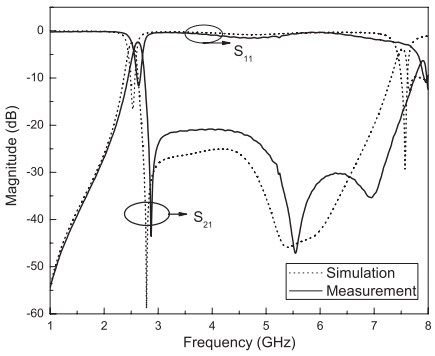

Figure 4. Simulated and measured S parameters of the proposed filter with second harmonic suppression.

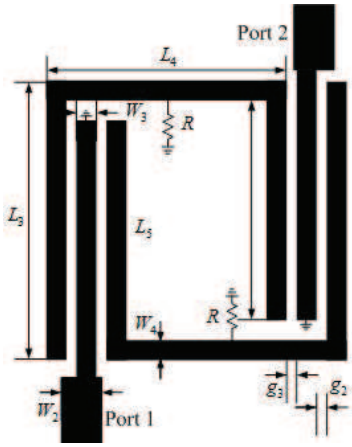

Figure 5. Configuration of the proposed filter with second, third and fourth harmonic suppression.

2.6 GHz against the simulated result of 2.5 GHz. The 3-dB bandwidth is from 2.52 GHz and 2.70 GHz, making the fractional bandwidth of 7%. The insertion loss, including the loss from subminiature A (SMA) connectors, is 2.4 dB compared to the simulated loss of 2.5 dB. As predicted, the second harmonic is suppressed by the special coupling region. The measured upper rejection band is increased up to near third-order harmonic and the rejection level during the stop-band is more than 20 dB.

3.2. Bandpass Filter with Second, Third and Fourth Harmonic Suppression

To improve the upper rejection band, another bandpass filter with the second-, third- and fourth-order harmonics suppression is designed in this section. The configuration of the proposed filter is shown in Fig. 5. It consists of two centrally-loaded half-wavelength resonators and two short-ended feed lines. The second special coupling region as shown in Fig. 1(b) is adopted to suppress the third harmonic. As discussed in [22], the second and fourth harmonics can be suppressed by loading resistors with value of 33 Ω at the center of the half-wavelength resonators. Therefore, upper rejection band is increased to near fifth-order harmonic.

The experimental filter is also fabricated on the substrate with

a relative dielectric constant $\epsilon_r = 2.33$ and thickness of 0.787 mm. The dimensions are shown as follows: $L_3 = 15$ mm, $L_4 = 15$ mm, $L_5 = 14$ mm, $W_2 = 2.3$ mm, $W_3 = 0.5$ mm, $W_4 = 0.5$ mm, $g_2 = 0.2$ mm, $g_3 = 0.2$ mm. The photograph of the proposed filter is illustrated in Fig. 6.

The simulation of this design is accomplished by using Ansoft HFSS. The fabricated prototype is measured by a ROHDE & SCHWARZ ZVA 50 network analyzer. The simulated and measured results are compared in Fig. 6. The center frequency of the passband is measured at 2.5 GHz. The 3-dB bandwidth is from 2.42 GHz and 2.56 GHz, making the fractional bandwidth of 5.6%. The insertion loss, including the loss from subminiature A (SMA) connectors, is 2.4 dB compared to the simulated loss of 1.3 dB, which can be attributed to the metal loss, substrate loss and fabrication error. At high frequency, some discrepancies are observed, which mainly due to the unexpected fabrication tolerance. However, Fig. 7 shows that the measured upper rejection band is increased up to fifth-order harmonic, and the rejection level during the stop-band is more than 20 dB.

3.3. Dual-band Bandpass Filter with Harmonic Suppression

Replacing the centrally-loaded resistors by capacitors, a novel dual-band bandpass filter can be designed as shown in Fig. 8. Based on the analysis presented in [22], odd-mode resonant frequencies can be

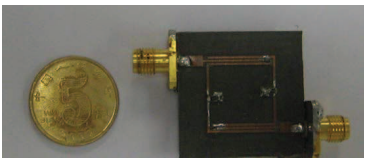

Figure 6. The photograph of the proposed filter with second, third and fourth harmonic suppression.

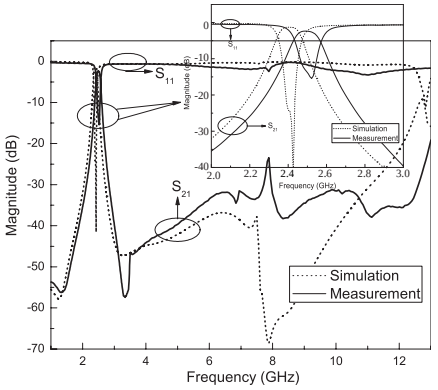

Figure 7. Simulated and measured S parameters of the proposed filter with wide upper rejection band.

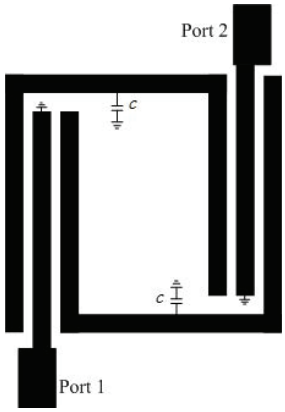

Figure 8. Structure of the proposed dual-band bandpass filter.

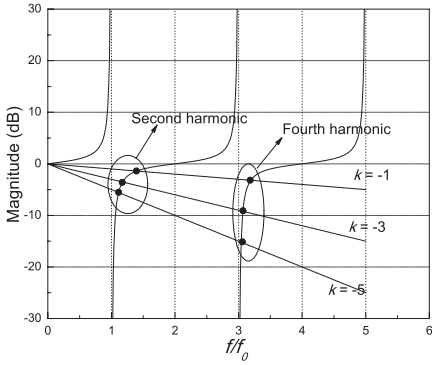

Figure 9. The locations of the even-mode resonant frequencies.

expressed as

$$f_{\text{odd}} = (2n-1)f_0 \tag{10}$$

where $n = 1, 2, 3, \ldots$, f_0 is the fundamental frequency of the centrally-loaded resonator. It is found that the loading capacitor has no impact on the odd-mode resonant frequencies.

For the even-mode resonance, the input admittance is given by

$$Y_{\text{in,even}} = jY\frac{\pi Cf + Y\tan\left(\dfrac{\pi}{2}\cdot\dfrac{f}{f_0}\right)}{Y - \pi Cf\cdot\tan\left(\dfrac{\pi}{2}\cdot\dfrac{f}{f_0}\right)} \tag{11}$$

Thus, the resonance condition $Y_{\text{in,even}} = 0$ becomes

$$k\frac{f}{f_0} = \tan\left(\frac{\pi}{2}\cdot\frac{f}{f_0}\right) \tag{12}$$

where,

$$k = -\frac{\pi Cf}{Y} \tag{13}$$

By tuning the values of centrally-loaded capacitance C, fundamental frequency f_0, and characteristic admittance Y, even-mode resonant frequencies can be controlled. As shown in Fig. 9, the locations of the even-mode resonant frequencies can simply be the intersections of the straight line kf/f_0 and the tangent curve. It is obvious that the fourth harmonic is shifted to near third one as

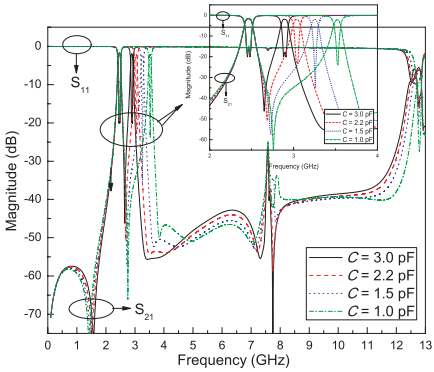

Figure 10. Simulated results against the centrally-loaded capacitance C.

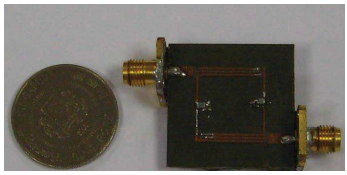

Figure 11. The photograph of the proposed dual-band bandpass filter with harmonic suppression.

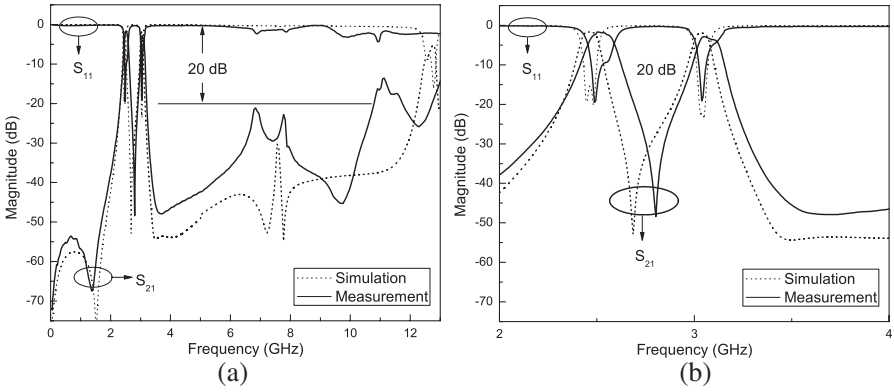

Figure 12. (a) Wide- and (b) narrow-band simulated and measured results of the proposed dual-band bandpass filter.

the value of centrally-loaded capacitor increases. Therefore, both the third- and fourth-order harmonics can be suppressed due to the special coupling region illustrated in Fig. 1(b). Simulated S parameters under different centrally-loaded capacitance are shown in Fig. 10.

To validate the proposed idea, a prototype is also implemented. The experimental filter is fabricated on the substrate with a relative dielectric constant $\epsilon_r = 2.2$ and thickness of 0.787 mm. The dimensions of the proposed dual-band filter are the same as them of the proposed filter in Section 3.2. The value of the centrally-loaded capacitance is 2.2 pF. The photograph of the proposed dual-band filter is shown in

Fig. 11.

The simulation of this design is accomplished by using Ansoft Designer. The fabricated prototype is measured by a ROHDE & SCHWARZ ZVA 50 network analyzer. Fig. 12 depicts the simulated and measured results, which shows good agreement. The lower passband is centered at 2.5 GHz and has a fractional bandwidth of 4.8%. The upper passband is centered at 3.05 GHz with a fractional bandwidth of 5.6%. The insertion losses of two passbands, including the loss from SMA connectors, are about 1.3 dB and 2.9 dB, respectively. The upper rejection band is increased up to near fifth harmonic and the rejection level is more than 20 dB.

4. CONCLUSION

In this paper, a novel class of microstrip bandpass filters with improved upper rejection band is proposed. Based on the voltage-wave analysis, we examine the coupling properties between the resonator and the feed line. Two special coupling regions are adopted to suppress the second and third harmonics, respectively. Using half-wavelength resonators with and without centrally-loaded resistors or capacitors, two single- band and one dual-band bandpass filters with improved upper rejection band are designed, simulated and measured. The simulated and measured results illustrate that the upper rejection bands of the proposed filters are increased up to third- and fifth-order harmonics, respectively. And the rejection level during the stop-bands is more than 20 dB.

ACKNOWLEDGMENT

This work is supported by the Fundamental Research Funds for the Central Universities under Projects 2011QNA5022.

REFERENCES

1. Gao, M.-J., L.-S. Wu, and J.-F. Mao, "Compact notched ultra-wideband bandpass filter with improved out-of-band performance using quasi electromagnetic bandgap structure," *Progress In Electromagnetics Research*, Vol. 125, 137–150, 2012.
2. Chaudhary, G., Y. Jeong, K. Kim, and D. Ahn, "Design of dual-band bandpass filter with controllable bandwidths using new mapping function," *Progress In Electromagnetics Research*, Vol. 124, 17–34, 2012.

3. Kuo, J.-T. and S.-W. Lai, "New dual-band bandpass filter with wide upper new rejection band," *Progress In Electromagnetics Research*, Vol. 123, 371–384, 2012.
4. Lopetegi, T., M. A. G. Laso, J. Hernandez, M. Bacaicoa, D. Benito, M. J. Garde, M. Sorolla, and M. Guglielmi, "New microstrip 'wiggly-line' filters with spurious passband suppression," *IEEE Microw. Theory and Tech.*, Vol. 49, No. 9, 1593–1598, 2001.
5. Kuo, J. T., W. H. Hsu, and W. T. Huang, "Parallel coupled microstrip filters with suppression of harmonic response," *IEEE Microw. Wireless Compon. Lett.*, Vol. 12, No. 10, 383–385, 2002.
6. Kim, B. S., J. W. Lee, and M. S. Song, "An implementation of harmonic-suppression microstrip filters with periodic grooves," *IEEE Microw. Wireless Compon. Lett.*, Vol. 14, No. 9, 413–415, 2004.
7. Kim, I. K., N. Kingsley, M. Morton, R. Bairavasubramanian, J. Papapolymerou, M. M. Tentzeris, and J. G. Yook, "Fractal-shaped microstrip coupled-line bandpass filters for suppression of second harmonic," *IEEE Microw. Theory and Tech.*, Vol. 53, No. 9, 2943–2948, 2005.
8. Wang, Y. X., B.-Z. Wang, and J. P. Wang, "A compact square loop dual-mode bandpass filter with wide stop-band," *Progress In Electromagnetics Research*, Vol. 77, 67–73, 2007.
9. Ye, C.-S., Y.-K. Su, M.-H. Weng, C.-Y. Hung, and R.-Y. Yang, "Design of the compact parallel-coupled lines wideband bandpass filters using image parameter method," *Progress In Electromagnetics Research*, Vol. 100, 153–173, 2010.
10. Kuo, J.-T., C.-Y. Fan, and S.-C. Tang, "Dual-wideband bandpass filters with extended stopband based on coupled-line and coupled three-line resonators," *Progress In Electromagnetics Research*, Vol. 124, 1–15, 2012.
11. Kuo, J.-T. and E. Shih, "Microstrip stepped impedance resonator bandpass filter with an extended optimal rejection bandwidth," *IEEE Microw. Theory and Tech.*, Vol. 51, No. 5, 1554–1559, 2003.
12. U-yen, K., E. J. Wollack, T. A. Doiron, J. Papapolymerou, and J. Laskar, "A planar bandpass filter design with wide stopband using double split-end stepped-impedance resonators," *IEEE Microw. Theory and Tech.*, Vol. 54, No. 3, 1237–1244, 2006.
13. Zhang, J., J.-Z. Gu, B. Cui, and X.-W. Sun, "Compact and harmonic suppression open-loop resonator bandpass with tri-section SIR," *Progress In Electromagnetics Research*, Vol. 69, 93–100, 2007.

14. Wu, Y.-L., C. Liao, and X.-Z. Xiong, "A dual-wideband bandpass filter based on E-shaped microstrip SIR with improved upper-stopband performance," *Progress In Electromagnetics Research*, Vol. 108, 141–153, 2010.
15. Kuo, J.-T., S.-C. Tang, and S.-H. Lin, "Quasi-electric function bandpass filter with upper stopband extension and high rejection level using cross-coupled stepped-impedance resonators," *Progress In Electromagnetics Research*, Vol. 114, 395–405, 2011.
16. Chen, C. F., T. Y. Huang, and R. B. Wu, "Design of microstrip bandpass filters with multiorder spurious-mode suppression," *IEEE Microw. Theory and Tech.*, Vol. 53, No. 12, 3788–3793, 2005.
17. Dai, G. L., X. Y. Zhang, C. H. Chan, Q. Xue, and M. Y. Xia, "An investigation of open- and short-ended resonators and their applications to bandpass filters," *IEEE Microw. Theory and Tech.*, Vol. 57, No. 9, 2203–2210, 2009.
18. Li, Y. C., X. Y. Zhang, and Q. Xue, "Bandpass filter using discriminating coupling for extended out-of-band suppression," *IEEE Microw. Wireless Compon. Lett.*, Vol. 20, No. 7, 369–371, 2010.
19. Zhang, X. Y. and Q. Xue, "Harmonic-suppressed bandpass filter based on discriminating coupling," *IEEE Microw. Wireless Compon. Lett.*, Vol. 19, No. 11, 695–697, 2009.
20. Hong, J.-S. and M. J. Lancaster, *Microstrip Filters for RF/Microwave Applications*, Wiley, New York, 2001.
21. Chen, C. Y. and C.-Y. Hsu, "A simple and effective method for microstrip dual-band filters design," *IEEE Microw. Wireless Compon. Lett.*, Vol. 16, No. 5, 246–248, 2006.
22. Zhang, X. Y. and Q. Xue, "Novel centrally loaded resonators and their applications to bandpass filters," *IEEE Microw. Theory and Tech.*, Vol. 56, No. 4, 913–921, 2008.